Effect of Combustion on the Frequency Response of Jets in Crossflow

Palash Sashittal*, Taraneh Sayadi†, Daniel Bodony‡
Department of Aerospace Engineering
University of Illinois at Urbana-Champaign, Urbana, IL 61801, USA

Peter Schmid§
Department of Mathematics
Imperial College London, London, SW7 2AZ, UK

I. Introduction

A jet in crossflow (JICF) describes a flow scenario where a transverse jet (reactive or non-reactive) impinges on a boundary layer. This flow configuration is considered as a benchmark, describing flows in many engineering applications such as fuel injectors and dilution holes in gas turbines, film cooling of turbine jets, control of boundarylayer separation, and dispersion of pollutants from smoke stacks, to name a few. Given its importance, JICF has been the subject of numerous experimental and numerical studies. Refs. [1, 2] summarize the different instabilities supported by the JICF, including whether they are characterized as convective, global or otherwise.

The majority of previous studies dedicated to characterizing the instability mechanisms of JICF have focused on the non-reacting case, where the jet to freestream velocity ratio R has been shown to play a crucial role as a destabilizing parameter. Megerian et. al. [3] performed experiments of JICF with different velocity ratios and observed a dramatic shift in the velocity spectra around $R \approx 3$ indicating a transition from convective to global instability. Instability analysis for a range of velocity ratios has also been undertaken by Ilak et. al. [4], with similar conclusions. The impact of combustion on JICF instabilities has not been explored.

Linear stability analysis of non-reacting JICF [5] using a global mode approach has offered valuable insight towards the dynamics of the flow. Using fully nonlinear direct numerical simulations (DNS) together with modal decomposition, employing global modes and proper orthogonal decomposition (POD), Ref. [6] demonstrated the presence of periodic oscillations in the absence of external forcing.

In this study, we study the global stability of non-reactive and reactive jets in crossflow to understand the impact of combustion on the observed JICF instabilities. We employ discrete adjoint framework of [7] to construct the adjoint solution of the forward reacting flow problem, which allows the analysis of the response behaviour to external harmonic forcing, but in a reactive context. The approach proposed by [7] is particularly efficient, since the discretized nonlinear operators and well-posed boundary conditions are readily available. The linearized operators are then derived by simply using the local differentiation technique described in [7] and without explicitly forming the respective matrices. This approach has been recently applied to an axisymmetric M-flame [8], where the inverse problem has allowed the investigation of the mechanism governing frequency response of the flame to the surrounding acoustic wave. The response

*Graduate Research Assistant, Department of Aerospace Engineering, University of Illinois at Urbana-Champaign, 306 Talbot Lab, 104 S. Wright St., Urbana, 61801, IL, USA, AIAA Student Member

†Adjunct Professor, Department of Aerospace Engineering, University of Illinois at Urbana-Champaign

‡Associate Professor, Department of Aerospace Engineering, University of Illinois at Urbana-Champaign, AIAA Associate Fellow

§Chair Professor of Applied Mathematics and Mathematical Physics, Department of Mathematics, Imperial College London, London, UK

behaviours of non-reacting and reacting jets in crossflow are compared to isolate the effect of combustion on the dynamics of the flow. Dynamic Mode Decomposition (DMD) is performed on the nonlinear simulation snapshots to extract the fundamental frequencies of the flow. These frequencies provide a guide to the range of frequencies to explore for the response of the linearized system for both the reacting and non-reacting case. Optimal forcing and response for the flows are found using adjoint based optimization. The variational formulation for the constrained optimization problem is adopted from [9].

The paper is structured as follows. In Sec. II, we describe the flow configuration and the governing equations of the flow. Sec. III outlines the method employed for the frequency response analysis and describes the mathematical formulation of the problem. The details of the numerical framework employed in the study are given in Sec. IV. Finally Sec. V shows the results and Sec. VI provides an outline of the future work.

II. Flow configuration

We consider a laminar transverse jet emerging in a crossflow boundary layer over a flat plate. The free-stream Mach number is $M = 0.2$ and the jet to free-stream velocity ratio defined using the maximum velocity in the jet is $R = 3$. From the experiments and previous simulations we expect the cold case [4, 5] to be globally unstable. The reference Reynolds number, based on the distance from the leading edge of the plate is $Re_{ref} = 10^4$. The reference distance x_{ref}, is taken as the distance from the leading edge such that $x/x_{ref} = Re_x/10^4$. The inlet of the computational domain is at $x_{inlet} = 0.7$ measured from the leading edge of the plate and the jet is located at the distance of $x_{jet} = 0.92$. The jet diameter is $D/x_{ref} = 0.0495$. The domain lengths in the streamwise, wall-normal and spanwise directions are 1.2, 0.4 and 0.5, respectively.

II.A. Governing equations

The compressible reactive Navier-Stokes equations are solved for the flow and reactive variables. In the reactive case, the Lewis number of all species is taken as unity $Le = 1$ and for simplicity the heat capacity is also assumed to be constant. The scalar diffusion is modeled by Fick's Law, resulting in the following system of equations,

$$\frac{\partial \rho}{\partial t} + \frac{\partial}{\partial x_j}(\rho u_j) = 0 \tag{1}$$

$$\frac{\partial \rho u_i}{\partial t} + \frac{\partial}{\partial x_j}(\rho u_i u_j + p\delta_{ij}) = \frac{\partial \sigma_{ij}}{\partial x_j} \tag{2}$$

$$\frac{\partial E}{\partial t} + \frac{\partial}{\partial x_j}[(E+p)u_j] = \dot{\omega}_T - \frac{\partial q_j}{\partial x_j} + \frac{\partial}{\partial x_k}(u_j \sigma_{jk}) \tag{3}$$

$$\frac{\partial \rho Y_k}{\partial t} + \frac{\partial (\rho u_j Y_k)}{\partial x_j} = -\dot{\omega}_f + \frac{\partial}{\partial x_j}\left[\frac{\nu}{Sc}\frac{\partial \rho Y_k}{\partial x_j}\right] \tag{4}$$

where,

$$\dot{\omega}_T = \Sigma_k \dot{\omega}_k \Delta h_k^0 \tag{5}$$

and $\rho, u_i, p, E, \sigma_{ij}$ and q_i are the non-dimensional density, velocity vector, pressure, total energy, viscous stress tensor and heat flux respectively. The parameter ν stands for the kinematic viscosity and Sc represents the Schmidt number, which is set to 0.7 for the duration of this study. Y_k is the mass fraction of each species. $\dot{\omega}_k$ denotes the production rate of species 'k' and Δh_k^0 is its respective heat of formation at some reference temperature T_0. In this case, a one-step combustion model with lean chemistry approximations [8] is adopted, leading to the following equations for $\dot{\omega}_T$ and $\dot{\omega}_f$

$$\begin{aligned} \dot{\omega}_f &= Da\, \rho^2 Y_f Y_o \exp\left(-\frac{Ze}{T}\right), \\ \dot{\omega}_o &= s\, \dot{\omega}_f \\ \dot{\omega}_T &= Ce\, \dot{\omega}_f, \end{aligned} \tag{6}$$

where Da is the Damköhler number, Ze is the Zeldovich number, Ce is the heat release parameter and s is the stoichiometric ratio. The above set of equations are closed using the equation of state,

$$p = \frac{\gamma - 1}{\gamma}\rho T \tag{7}$$

where p, γ and T are pressure, specific heat ratio and temperature of the fluid respectively.

III. Frequency response analysis

The response of reacting and non-reacting jets in crossflow to small amplitude harmonic forcing is analyzed by considering the finite time response of governing equations linearized about the steady state solution.The range of frequencies to study is chosen by looking at the dominant frequencies in the nonlinear flow regime. These frequencies are extracted by means of Dynamic Mode Decomposition (DMD) [10, 11, 12]. For each extracted frequency, the optimal forcing function that maximizes the growth in the energy norm is determined using the adjoint based method.

III.A. Mathematical formulation

In this section, the mathematical formalism to find the optimal forcing that maximizes an objective function is outlined. Finite time response of linearized governing equations discretized in space and harmonically forced are considered. The forward/direct equation constitutes the evolution of the state variables, $\mathbf{q}$, forward in time defined by,

$$\frac{d\mathbf{q}}{dt} = \mathbf{A}\mathbf{q} + \mathbf{B}\mathbf{f}sin(\omega t) = R(\mathbf{q}, \mathbf{f}, \omega), \quad \mathbf{q}(0) = 0, \tag{8}$$

where $A = \frac{\partial \mathbf{F}}{\partial \mathbf{q}}\Big|_{\bar{\mathbf{q}}}$ with $\mathbf{F}$ representing the discrete nonlinear equations that govern the state variables and $\mathbf{f}$ denoting the forcing function. The system is being forced with frequency ω and $\bar{\mathbf{q}}$ is the base solution about which the governing equations are linearized. An objective function J of the form,

$$J(\mathbf{q}) = \phi(\mathbf{q}(T_f)) + \int_0^T \psi(\mathbf{q}(t))dt \tag{9}$$

is considered, where ϕ is the contribution from the terminal state to the objective function at time T_f and ψ accounts for its integral contribution. Using this objective functional, the Lagrange functional L is formulated as,

$$L(\mathbf{q}, \mathbf{f}, \omega, \boldsymbol{\eta}, \xi) = J(\mathbf{q}) - \int_0^T \boldsymbol{\eta} \cdot \left(\frac{d\mathbf{q}}{dt} - R(\mathbf{q}, \mathbf{f}, \omega)\right) dt - \xi(\mathbf{f} \cdot \mathbf{f} - 1) \tag{10}$$

For the optimal forcing at a given frequency, the norm described by the inner product $\langle \mathbf{u}, \mathbf{v} \rangle = \mathbf{v}^\top \mathbf{D}\mathbf{u}$ is maximized. $\mathbf{D}$ represents a symmetric positive-definite mass matrix that accounts for the volume integral of the discretized domain. Hence, in the description of the objective function, $\phi(\mathbf{q}(T_f)) = \langle \mathbf{q}(T_f), \mathbf{q}(T_f) \rangle$ and $\psi(\mathbf{q}(t)) = 0$. Setting the variation of the Lagrange functional with respect to the state variables to zero leads to the adjoint equation defined by

$$-\frac{d\boldsymbol{\eta}}{dt} = \left(\frac{\partial R}{\partial \mathbf{q}}\right)^\top \boldsymbol{\eta}, \quad \boldsymbol{\eta}(T_f) = 2\mathbf{D}\mathbf{q}(T_f), \tag{11}$$

It can be deduced from Eq. (11), the equation governing the evolution of the adjoint variable is initialized by the solution of the direct system, $\mathbf{q}$. The optimality condition is given by setting the variation with respect to the forcing function to zero,

$$\mathbf{f} = \frac{1}{2\xi} \int_0^T \mathbf{B}^\top \boldsymbol{\eta} sin(2\pi\omega t)dt \tag{12}$$

where ξ turns out to be the normalizing constant for $\mathbf{f}$. Solving the adjoint equations together with the constraints in one-step, is computationally very expensive, therefore an iterative approach is adopted here. The algorithm is summarized as,

1. Given the n^{th} guess of forcing function $\mathbf{f}^n$, solve the direct equation Eq. 8 forward in time
2. Use the direct solution to initialize and solve the adjoint equation Eq. 11 backward in time
3. Use the adjoint solution to update the forcing function $\mathbf{f}^{n+1}$ using Eq. 12
4. Continue until change in objective function is less than some threshold.

IV. Numerical approach

A direct numerical simulation is performed using a modified version of the solver developed by [13] and [14], where the compressible Navier-Stokes equations, including reactions, are solved. An explicit third-order Runge-Kutta scheme is used for time stepping. The spatial discretization is on a structured curvilinear grid with staggered variables in space. In the reactive case, due to the stiffness of the chemical reactions, operator-splitting technique is adopted, where combustion source terms are solved using a 5^{th} order backward differentiation method [15].

IV.A. Boundary conditions

The velocity profile at the inlet of the jet (see Fig. 1) is prescribed using an inhomogeneous boundary condition for the wall-normal velocity at the plate [5]. Similar to the velocity profile, a temperature distribution satisfying the pipe Poiseuille flow is used at the inflow of the jet. Isothermal wall boundary conditions are used everywhere else on the plate. Periodic boundary conditions are employed along the spanwise and streamwise directions. To account for the spatially growing boundary layer in a streamwise periodic domain, the profile is reshaped and re-scaled at the end of the domain to a similarity solution of a laminar compressible boundary layer at the inflow. Sponges are used at all the boundaries except for the wall boundary to ensure nonreflective inflow and outflow.

IV.B. Base flow computation

The system is linearized about the steady state solution $\bar{\mathbf{q}}$ of the nonlinear governing equations. The steady state solution is determined by the use of selective frequency damping (SFD) [16], where the following system of equations are solved until convergence is achieved,

$$\frac{d\mathbf{q}}{dt} = f(\mathbf{q}, \mathbf{g}) - \chi(\mathbf{q} - \bar{\mathbf{q}}), \tag{13}$$

$$\frac{d\bar{\mathbf{q}}}{dt} = \frac{(\mathbf{q} - \bar{\mathbf{q}})}{\Delta}. \tag{14}$$

Here, χ and Δ are user-defined filter parameters that control the filter width and cutoff frequency of the filter.

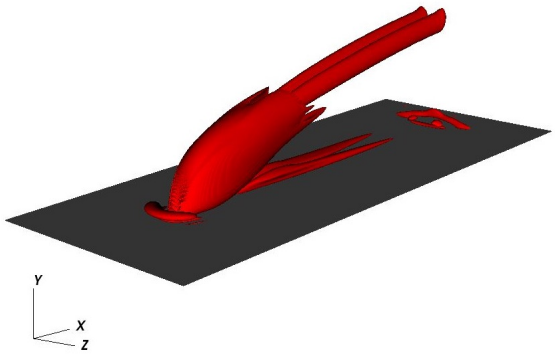

(a)

Figure 1: Base flow with red iso-surfaces of Q criterion for the non-reacting jet in crossflow. The grey surface depicts the flat plate.

Figure 1 shows the base flows of the non-reacting jet in crossflow using iso-surfaces of Q criterion as an indicator of vortical structures in the flow. The counter-rotating vortex pair (CVP) is observed along the jet trajectory.

V. Non-reacting JICF Results

V.A. Frequency selection

Dynamic mode decomposition is used to extract coherent structures with a single temporal frequency from a sequence of data snapshots [10]. Previous studies have shown that the fundamental frequencies, pertaining to self-sustained oscillations in the flow, are related to the region near the inlet of the jet [6]. Therefore, we limit our series of snapshots for both cases to the region near the inlet. This region comprises the shear layer upstream of the jet inlet and the separation region behind the inlet in the wake of the jet. To recognize the most influential modes in the flow, a sparsity promoting DMD algorithm is employed [11].

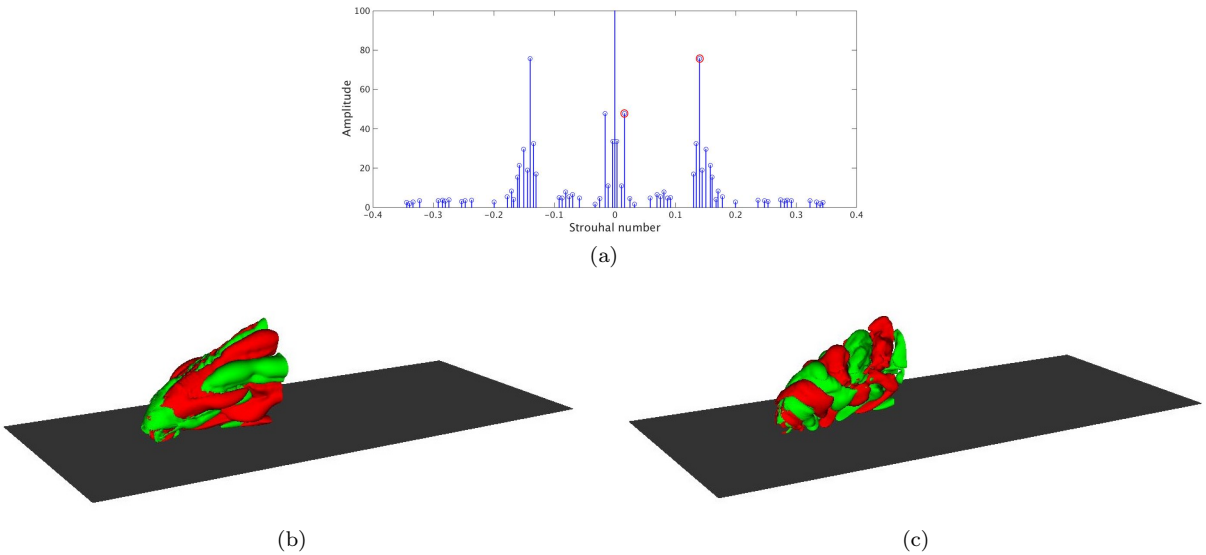

(a)

(b) (c)

Figure 2: (a) Spectra of the dynamical modes for the non-reacting case selected by sparsity promoting algorithm. The dominant frequencies are highlighted by red markers. Spatial modes at frequencies (b) $St - 0.016$ and (c) $St = 0.14$ for the non-reacting jet in crossflow. The red and green isocontours depict positive and negative wall normal velocity, respectively. The grey surface represents the flat plate.

Figure 2a shows the dominant frequencies and their respective amplitudes in the nonlinear non-reacting jet in crossflow. Clear peaks at $St = 0.14$ and $St = 0.016$ are observed which correspond shear layer vortices and wall vortices respectively and are both initiated by the seperation region just downstream of the jet inlet [6]. The extracted frequenceis agree well with the previous studes on non-reacting jets in crossflow for comparable velocity ratios [4, 5]. The associated spatial modes are shown in figure 2b and 2c.

Using the extracted frequencies as a guide, 10 frequencies within the St range $[0.04, 0.08]$ and $[0.1, 0.18]$ are selected and frequency response analysis will be performed for each frequency for both reactive and non-reactive jets. Knowing the optimal gain and its gradient at these frequencies will enable us to create a frequency map of the response of the flows to harmonic forcing.

V.B. Response to harmonic forcing

In this section we look at the optimal forcing structure and response for non-reacting case for the frequency $St = 0.05$. The terminal time T_f is chosen as 2.8 times the time period of the forcing oscillation.

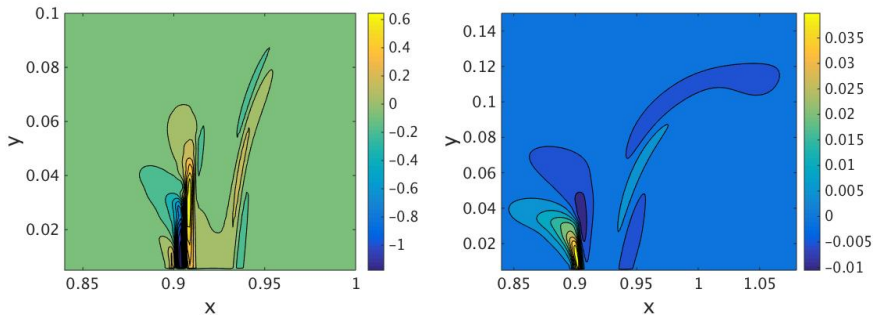

(a) (b)

Figure 3: (a) Optimal forcing function and (b) optimal response of non-reacting jet in crossflow at $St = 0.05$ on the symmetry plane.

Figure 3 shows the optimal forcing and response for the non-reacting jet in crossflow at $St = 0.05$. The forcing lies in the shear layer just upstream of the jet inlet which is centered at $x_{jet} = 0.92$. The response on the other hand, lies around the counter-rotating vortex pair of the base flow. This is expected since the flow exhibits convective instability for the flow parameters under consideration.

VI. Future Work

The aim of this study is to understand the effect of combustion on the frequency selection mechanisms in jet in crossflow. To that end, we compare the response of non-reacting and reacting jets in comparable flow conditions to harmonic forcing. The range of frequencies for the forcing is determined by the fundamental frequencies of the nonlinear simulations of the jets in crossflow. Dynamic Mode Decomposition (DMD) is employed to extract the dominant frequencies from a sequence of data snapshots for both the non-reacting and reacting jets. Frequencies obtained from DMD of non-reacting case matches perfectly with previous studies. Reacting jet in crossflow simulations will be performed with comparable flow parameters to the non-reacting case. The fundamental frequencies of the reacting case will reveal the role of combustion in the stability of the flow.

Adjoint based optimization framework is being used to find the optimal response and optimal forcing function for both reacting and non-reacting cases. Optimal gain from forcing at $St = 0.05$ for the non-reacting case has been computed. Similar computations of optimal gain for more frequencies will provide a frequency map of gain for both cases. This will shed light on how combustion influences the response of the jets to forcing at different frequencies.

Acknowledgments

The authors would like to thank Prof. Vincent Le Chenadec for numerous fruitful discussions. The authors also acknowledge the use of computational resources from the Bluewaters cluster awarded by the National Center for Supercomputing Applications.

References

[1] Ann R Karagozian. Transverse jets and their control. *Prog. Energ. Combust.*, 36(5):531–553, 2010.

[2] Krishnan Mahesh. The interaction of jets with crossflow. *Annual Review of Fluid Mechanics*, 45:379–407, 2013.

[3] Sevan Megerian, J Davitian, LS de B Alves, and AR Karagozian. Transverse-jet shear-layer instabilities. part 1. experimental studies. *Journal of fluid Mechanics*, 593:93–129, 2007.

[4] M. Ilak, P. Schlatter, S. Bagheri, and D. S Henningson. Bifurcation and stability analysis of a jet in cross-flow: onset of global instability at a low velocity ratio. *J. Fluid Mech.*, 696:94–121, 2012.

[5] Shervin Bagheri, Philipp Schlatter, Peter J Schmid, and Dan S Henningson. Global stability of a jet in crossflow. *J. Fluid Mech.*, 624:33–44, 2009.

[6] Philipp Schlatter, Shervin Bagheri, and Dan S Henningson. Self-sustained global oscillations in a jet in crossflow. *Theoretical and Computational Fluid Dynamics*, 25(1-4):129–146, 2011.

[7] Miguel Fosas De Pando, Denis Sipp, and Peter J Schmid. Efficient evaluation of the direct and adjoint linearized dynamics from compressible flow solvers. *J. Comput. Phys.*, 231(23):7739–7755, 2012.

[8] M. Blanchard, T. Schuller, D. Sipp, and P. J. Schmid. Response analysis of a laminar premixed M-flame to flow perturbations using a linearized compressible Navier-Stokes solver. *Phys. Fluids*, 27(4):043602, 2015.

[9] Carlo Cossu. An introduction to optimal controllecture notes from the flow-nordita summer school on advanced instability methods for complex flows, stockholm, sweden, 2013. *Appl. Mech. Rev.*, 66(2):024801, 2014.

[10] Peter J Schmid. Dynamic mode decomposition of numerical and experimental data. *Journal of fluid mechanics*, 656:5–28, 2010.

[11] Mihailo R Jovanović, Peter J Schmid, and Joseph W Nichols. Sparsity-promoting dynamic mode decomposition. *Physics of Fluids*, 26(2):024103, 2014.

[12] Taraneh Sayadi and Peter J Schmid. Parallel data-driven decomposition algorithm for large-scale datasets: with application to transitional boundary layers. *Theoretical and Computational Fluid Dynamics*, 30(5): 415–428, 2016.

[13] Santhanam Nagarajan, Sanjiva K Lele, and Joel H Ferziger. A robust high-order compact method for large eddy simulation. *J. Comput. Phys.*, 191(2):392–419, 2003.

[14] Taraneh Sayadi, Curtis W Hamman, and Parviz Moin. Direct numerical simulation of complete h-type and k-type transitions with implications for the dynamics of turbulent boundary layers. *J. Fluid Mech.*, 724:480–509, 2013.

[15] P. N. Brown, G. D. Byrne, and A. C. Hindmarsh. VODE: A variable-coefficient ODE solver. *SIAM J. Sci. Stat. Comp.*, 10(5):1038–1051, 1989.

[16] Espen Åkervik, Jérôme Hoepffner, Uwe Ehrenstein, and Dan S Henningson. Optimal growth, model reduction and control in a separated boundary-layer flow using global eigenmodes. *J. Fluid Mech.*, 579: 305–314, 2007.